Organic LETTERS

Letter

pubs.acs.org/OrgLett

Tetraphenylhexaazaanthracenes: 16π Weakly Antiaromatic Species with Singlet Ground States

Christos P. Constantinides, Georgia A. Zissimou, Andrey A. Berezin, Theodosia A. Ioannou, Maria Manoli, Demetra Tsokkou, Eleni Theodorou, Sophia C. Hayes, and Panayiotis A. Koutentis*

Department of Chemistry, University of Cyprus, P.O. Box 20537, 1678 Nicosia, Cyprus

Supporting Information

ABSTRACT: Tetraphenylhexaazaanthracene, **TPHA-1**, is a fluorescent zwitterionic biscyanine with a closed-shell singlet ground state. **TPHA-1** overcomes its weak 16π antiaromaticity by partitioning its π system into 6π positive and 10π negative cyanines. The synthesis of **TPHA-1** is low yielding and accompanied by two analogous TPHA isomers: the deep red, non-charge-separated, quinoidal **TPHA-2**, and the deep green **TPHA-3** that partitions into two equal but oppositely charged 8π cyanines. The three TPHA isomers are compared.

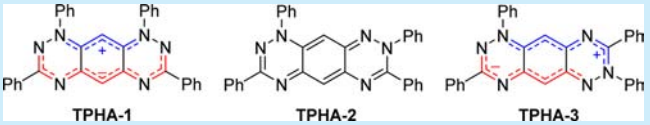

Organic polyacenes have uses in electronic devices.[1] Their extended π-electron-rich systems, tight solid-state packing, and short intermolecular interactions result in high hole mobility. These characteristics lead to their use as the active component in organic field-effect transistors (OFETs).[2] While the majority of all-carbon polyacenes demonstrate p-type conductivity, efficient n-type OFETs are not yet developed. Replacement of sp^2 carbons with nitrogens leads to n-type electron-deficient molecules. As such, aza-rich acenes are intensively pursued as building blocks for n-type conductors.[3] A subclass of azaacenes possesses zwitterionic structures comprising two independent cationic and anionic cyanine subunits.[4] The first modern derivative of this class of azaacenes, tetraphenylhexaazaanthracene, **TPHA-1**, was prepared by Wudl and is fluorescent.[4a]

Wudl's synthesis of **TPHA-1** involved the reaction of *N*,*N*′-(*m*-phenylene)dibenzimidoyl dichloride **1** with $PhNHNH_2$ to give the isolable but reportedly unstable bisamidrazone **2** that then oxidatively cyclized in the presence of DBU to afford **TPHA-1** in an overall yield of 17% (Scheme 1).

Oxidative cyclization of amidrazones into benzotriazinyls can be high yielding,[5] particularly when the starting amidrazones are pure. Despite several efforts, which involved screening various oxidants (see Supporting Information, SI), we failed to significantly improve on this yield. This led us to isolate and identify minor side products to help explain the low yield. Herein, we identify two of these as **TPHA-2** and **TPHA-3** which are isomers of **TPHA-1** (Figure 1).

Scheme 1. Wudl's Synthesis of TPHA-1

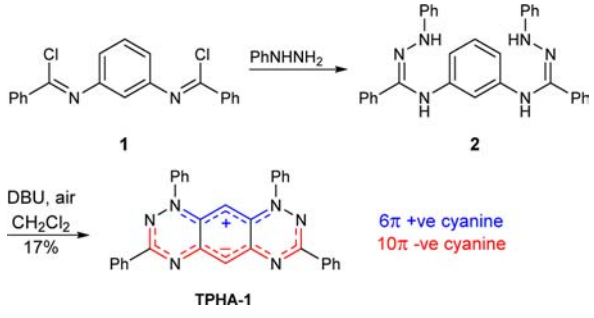

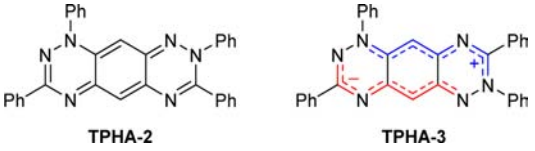

Figure 1. Structures of TPHA isomers.

Furthermore, we also purify and fully characterize the bisamidrazone **2**, enabling a quantitative conversion to **TPHA-1**, and provide an unambiguous alternative synthesis of **TPHA-1**.

Formation of these isomers can be rationalized: Wudl's bisamidrazone **2** synthesis follows the method of Potts et al.,[6] who reacted *N*-phenylbenzimidoyl chloride with $PhNHNH_2$ and noted that the reaction was not selective: $PhNHNH_2$ attacks via both α and β nitrogens to give a mixture of *N*′,*N*″- and *N*,*N*′-diphenylbenzamidrazones (see Scheme S1 in SI) that can be separated by extracting the reaction mixture with dilute acetic acid. The Potts workup, when applied to Wudl's bisamidrazone **2**, provides a mixture of bisamidrazones stemming from $PhNHNH_2$ attacking via both α and β nitrogens. We note that the spectroscopic data reported by Wudl for the bisamidrazone **2** was insufficient to determine both purity and structure.[4a] In our hands, rapid dry flash column chromatography of this mixture provided 28% of pure bisamidrazone **2**, which on treatment with Ag_2O (2.2 equiv)

Received: July 5, 2015
Published: August 5, 2015

DOI: 10.1021/acs.orglett.5b01923
Org. Lett. 2015, 17, 4026–4029

in DCM at 20 °C for 24 h gave **TPHA-1** in 98% yield (Scheme 2).

Scheme 2. Synthesis of TPHA-1 from Pure Bisamidrazone 2

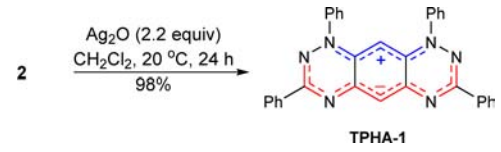

As such, **TPHA-2** must arise from a bisamidrazone **3** that results from one $PhNHNH_2$ attacking via the α and another attacking via the β nitrogens (Scheme 3). **TPHA-3**, which has

Scheme 3. Bisamidrazone Intermediates 3 and 4

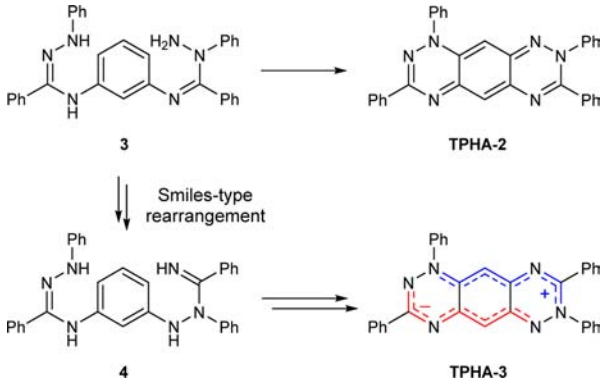

a clearly different C/N connectivity, presumably arises via a Smiles-type rearrangement[7] of intermediate **3** to intermediate **4** (or an oxidation product thereof; see Scheme S2 in SI). Our attempts to isolate or synthesize intermediate **3** or **4** failed. Nevertheless, we developed an alternative route to **TPHA-1** (Scheme 4). N-Nitroarylation of *N*′-phenylbenzohydrazide (**6**) via nucleophilic aromatic substitution of 1,5-difluoro-2,4-dinitrobenzene (**5**) afforded the bishydrazide **7**. Mild reduction with H_2 over Pd/C in EtOH and further thermal oxidative cyclization under acid catalysis affords only **TPHA-1** in an overall yield of 63%. This synthesis was based on our route to benzo- and pyrido-fused 1,2,4-triazinyl radicals, which avoids the need for moisture-sensitive imidoyl chlorides and difficult to isolate and purify bisamidrazones.[8]

Scheme 4. Unambiguous Route to TPHA-1

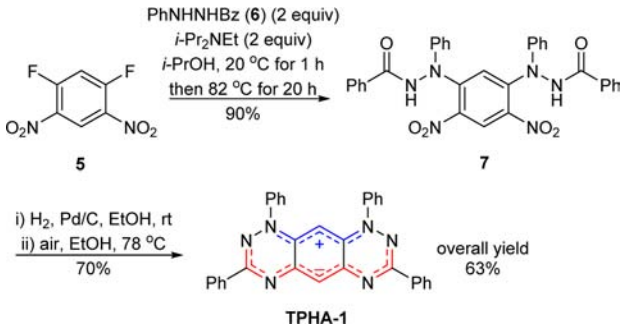

TPHA-2 and **TPHA-3** are air and thermally stable compounds (up to ~285 °C by DSC; see SI, section S8). They are EPR-silent and exhibit sharp line ^1H and ^{13}C NMR spectra, indicating a closed-shell electronic ground state despite their 16π antiaromatic periphery. They are moderately soluble in most organic solvents and can be recrystallized from PhH or EtOH to give single crystals. X-ray crystallography supported the quinoid structure for **TPHA-2** (CCDC-1062989) and the zwitterionic structure for **TPHA-3** (CCDC-1062988) (see Figures S1−S3 and Table S3 in SI). Nevertheless, an electrostatic surface potential plot shows considerable charge polarization even in **TPHA-2** (Figure 3); as such, the quinoid motif may not account fully for its ground-state structure. Crystal packing of **TPHA-1** (CCDC-1062987) shows molecules arranged in π stacks along the *ac* diagonal (Figure S4 in SI). The molecules are related through a center of inversion that places positive and negative cyanines opposite each other with $\pi-\pi$ stacking distances of ~3.42 Å. Conversely, for **TPHA-3**, zwitterionic molecules are packed in 1D regular chains along the *ac* diagonal (Figure S5 in SI). The molecules are related through translation and are equidistant at 3.70 Å. DFT calculations, at the UB3LYP/6-311G(2d) level of theory, closely matched the crystallographic geometries and enabled a study of their electronic nature.

A number of symmetrical and nonsymmetrical zwitterionic biscyanines have been reported.[4f,9] **TPHA-1** and 3,5,7,9-tetraphenylhexaazaacridine are the only examples of symmetrical zwitterionic biscyanines in the family of azaacenes, where the partition of the π system between the two cyanines is complete.[4a,d] While the 16π periphery in **TPHA-1** partitions to a 6π positive and 10π negative biscyanine, **TPHA-3** is unique in that it partitions equally to two oppositely charged 8π cyanines. This different electron distribution among the two cyanines is reflected in the distinct optical properties of these two isomers. Both **TPHA-1** and **TPHA-3** show pronounced negative solvatochromism typical of zwitterionic biscyanines (Figure 2). For the latter, a steeper slope of its

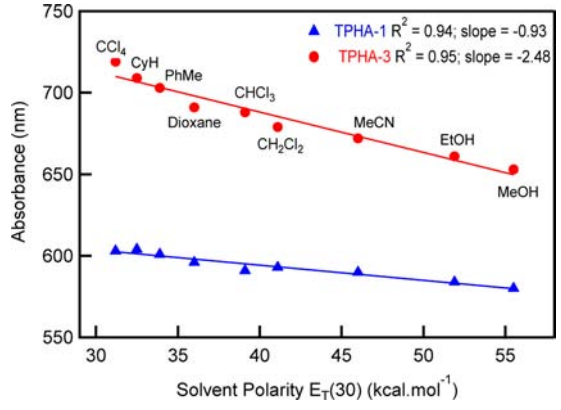

Figure 2. TPHA-1 and **TPHA-3** $\pi-\pi^*$ absorption vs solvent polarity $E_T(30)$. The solvent dependence of the 0−0 vibronic transition in the lowest energy band is displayed.

transition energy versus $E_T(30)$ plot denotes greater sensitivity to solvent polarity, which can be attributed to a larger difference between the ground- and excited-state dipole moment of **TPHA-3**. No solvatochromism was observed for **TPHA-2**, indicating that the difference between the ground- and excited-state dipole moment must be marginal (see SI Table S5).

To further study the charge separation, we calculated and compared the dipole's magnitude and vector for all of the isomers using geometries taken from full optimizations of the

DOI: 10.1021/acs.orglett.5b01923
Org. Lett. 2015, 17, 4026−4029

singlet states at the UB3LYP/6-311G(2d) level of theory (Figure 3). The symmetrical biscyanine **TPHA-1** has a dipole

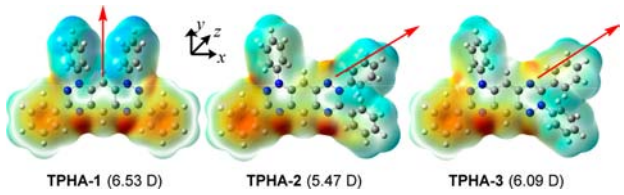

Figure 3. Calculated dipole moments of **TPHA-1**–**TPHA-3** (red arrow); electrostatic potential mapped on the electron density surface of **TPHA-1**–**TPHA-3**. Red = –ve electron density, blue = +ve electron density.

moment (6.53 D) that runs parallel to the direction of the positve to negative charge polarization (i.e., the *y* axis). The calculated dipole moment for **TPHA-3** aligns with the diagonal of the *x*–*y* plane, and its magnitude (6.09 D) confirms the high polarity of its ground state. Interestingly, **TPHA-2** has a similar diagonal dipole alignment with a relatively high moment (5.47 D) denoting the contribution of zwitterionic resonance structures in its ground state. TD-DFT calculations of the excited-state dipole moments fully agree with the change in dipole moment predicted from the solvatochromism plots (see Table 2 and SI Table S5).

UV–vis absorption spectroscopy highlights the different electron distributions among the TPHA isomers (Figure 4).

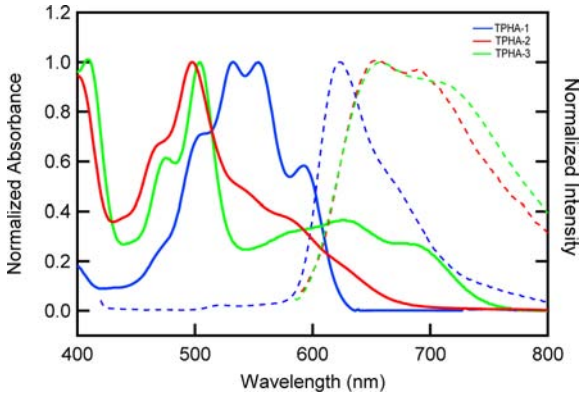

Figure 4. Absorbance (solid line) and PL (dashed line) spectra of **TPHA-1**–**TPHA-3** in DCM [λ_{exc} = 473 (**TPHA-1**) and 575 nm (**TPHA-2** and **TPHA-3**)] (for additional discussion, see section S5.1 and Figure S7 in SI).

TPHA-2 and **TPHA-3** possess two absorption bands in the visible range, which correspond to the HOMO–LUMO and the HOMO–LUMO+1 transitions, while **TPHA-1** has one main band with a 0–0 transition at 589 nm. The lowest energy transition is significantly red-shifted in **TPHA-2** and **TPHA-3** (624 and 687 nm, respectively) and agrees with the smaller calculated HOMO–LUMO gap (ΔE_{HL} = 2.15 and 1.84 eV, respectively, vs 2.30 eV for **TPHA-1**).

Spatial distribution of the frontier orbitals for **TPHA-1** and **TPHA-3** reveals subtle differences (Figure 5). The molecular orbitals of the TPHA isomers can be constructed using the 1,2,4,5-tetramethylenebenzene approach, that is, two radical fragments with nonequivalent odd number of π electrons (differ by $2e^-$) connected via σ bonds.[10] The zwitterion can be envisaged to form by transfer of an electron from the

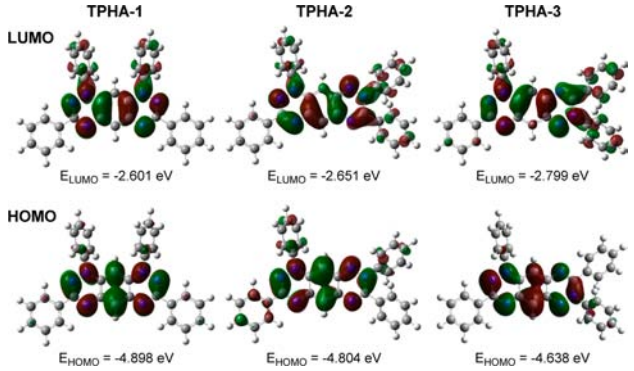

Figure 5. HOMO and LUMO orbitals of TPHA isomers [UB3LYP/6-311G(2d)].

donor to the acceptor radical fragment, leading to two new cyanines of equal π electron count. In contrast to that of **TPHA-1**, the HOMO orbital of **TPHA-3** is higher in energy, stemming from an increased orbital density on the *N*-imine acceptor fragment, that is, the positve cyanine (see orbital coefficients in Figure S6 in SI). The LUMO orbital of **TPHA-3** is more concentrated on the *N*-amino donor fragment, that is, the positive cyanine resulting in its stabilization compared to the LUMO of **TPHA-1** (see orbital coeffiecients in Figure S8 in SI). These two changes led to a smaller ΔE_{HL} for **TPHA-3** as reflected in the observed red shift.

The two charged conjugated cyanines in the symmetrical π antibonding HOMO of **TPHA-3** are connected via nodal carbons (i.e., no π electron density) (Figure 5). The crystal structure of **TPHA-3** shows that the cyanines are connected by longer C–C bonds [1.442(3)–1.459(3) Å]. The increased σ character of these bonds along with the bond equalization within the cyanines supports the presence of a zwitterionic biscyanine ground state. Nucleus independent chemical shift (NICS)[11] values of the TPHAs' individual rings support the central benzene (ring B) being weakly aromatic and the peripheral triazine rings being mildly antiaromatic (Table 1).

TPHA-1 and **TPHA-3** are "potentially antiaromatic". The lowest triplet state results from a single $\pi \rightarrow \pi^*$ excitation from the HOMO to the LUMO. Population of the LUMO with one electron breaks the separation between the two cyanines by providing the lateral C–C carbons with π bonding character and shorter bond lengths (Figure 5), restoring π delocalization and antiaromaticity.[12] The small calculated ΔE_{ST} values (–0.77, –0.86, and –0.72 eV for **TPHA-1**–**TPHA-3**, respectively) tentatively suggest that these materials may undergo singlet fission.[13]

All isomers exhibit broad PL in the visible region that is Stokes-shifted with respect to the absorbance peak (Figure 4). Under similar experimental conditions (pump fluence, diameter, and accumulation time), the PL signals from **TPHA-2** and **TPHA-3** were orders of magnitude weaker than that from **TPHA-1** when excited within the most intense absorption band. The latter has a quantum yield of 0.0995 ± 0.005, which differs from the reported value of Hutchison et al.[4a] (Table 2; see SI section S5 for discussion). Excitation of **TPHA-2** and **TPHA-3** within the HOMO–LUMO band enhanced the intensity of the PL; however, the Φ_f remained insignificant.

In conclusion, two new TPHA isomers were studied by X-ray diffraction, UV–vis and fluorescence spectroscopy, and DFT computations. **TPHA-3** is the first example of a

DOI: 10.1021/acs.orglett.5b01923
Org. Lett. 2015, 17, 4026–4029

Table 1. NICS(0), (1), and (−1) for Rings A, B, and C Calculated at the UB3LYP/6-311G(2d) Level of Theory

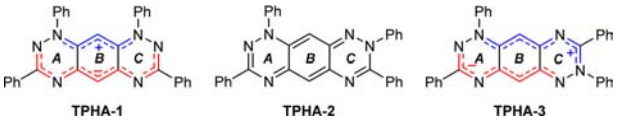

	TPHA-1			TPHA-2			TPHA-3		
ring	A	B	C	A	B	C	A	B	C
NICS(0)	8.8	1.2	8.8	9.9	2.2	8.9	12.0	2.5	10.8
NICS(1)	3.1	−2.1	3.2	4.0	−1.8	2.9	5.8	−1.6	4.8
NICS(−1)	3.1	−2.6	3.1	3.9	−1.2	3.5	5.6	−1.2	4.2

Table 2. Absorption [λ_{max}(abs) (log ε)], Optical Band Gap [E_g^{onset}], Fluorescence [λ_{max}(PL)] Maxima, and Quantum Yield (Φ_f) of TPHA-1−TPHA-3 in DCM

	λ_{0-0}(abs) (log ε) [nm]	E_g^{onset} (eV)	λ_{max}(PL) [nm]	Φ_f (λ_{exc} = 473 nm)
TPHA-1	589 (4.23)	1.62	622	0.0995 ± 0.005
TPHA-2	496 (4.35), 624 (3.48)	1.52	653	<0.002
TPHA-3	503 (4.32), 687 (3.66)	1.35	655	<0.008

zwitterionic azaacene with the π system split into two equal cyanines. This electron distribution leads to a smaller red-shifted HOMO−LUMO gap. Although the fluorescence quantum yield of **TPHA-3** is less than that of other azaacenes, the tight crystal packing and the smaller HOMO−LUMO gap indicate a promising direction to n-type materials for OFET applications, while the low ΔE_{ST} value suggests potential singlet fission properties.

■ ASSOCIATED CONTENT

Supporting Information

The Supporting Information is available free of charge on the ACS Publications website at DOI: 10.1021/acs.orglett.5b01923.

Experimental, computational, and spectroscopic characterization data (PDF)
TPHA-1 (CIF)
TPHA-2 (CIF)
TPHA-3 (CIF)

■ AUTHOR INFORMATION

Corresponding Author

*E-mail: koutenti@ucy.ac.cy.

Notes

The authors declare no competing financial interest.

■ REFERENCES

(1) (a) Anthony, J. E. *Chem. Rev.* **2006**, *106*, 5028. (b) Bendikov, M.; Wudl, F.; Perepichka, D. F. *Chem. Rev.* **2004**, *104*, 4891. (c) Anthony, J. E.; Facchetti, A.; Heeney, M.; Marder, S. R.; Zhan, X. *Adv. Mater.* **2010**, *22*, 3876.
(2) Sun, S.; Dalton, L. R. *Introduction to Organic Electronic and Optoelectronic Materials and Devices*; CRC: London, 2008.
(3) (a) Bunz, U. H. F. *Pure Appl. Chem.* **2010**, *82*, 953. (b) Bunz, U. H. F. *Chem.—Eur. J.* **2009**, *15*, 6780. (c) Richards, G. J.; Hill, J. P.; Mori, T.; Ariga, K. *Org. Biomol. Chem.* **2011**, *9*, 5005.
(4) (a) Hutchison, K.; Srdanov, G.; Hicks, R.; Yu, H.; Wudl, F.; Strassner, T.; Nendel, M.; Houk, K. N. *J. Am. Chem. Soc.* **1998**, *120*, 2989. (b) Wudl, F.; Koutentis, P. A.; Weitz, A.; Ma, B.; Strassner, T.; Houk, K. N.; Khan, S. I. *Pure Appl. Chem.* **1999**, *71*, 295. (c) Koutentis, P. A. *ARKIVOC* **2002**, *6*, 175. (d) Langer, P.; Bodtke, A.; Saleh, N. N. R.; Görls, H.; Schreiner, P. R. *Angew. Chem., Int. Ed.* **2005**, *44*, 5255. (e) Langer, P.; Amiri, S.; Bodtke, A.; Saleh, N. N. R.; Weisz, K.; Görls, H.; Schreiner, P. R. *J. Org. Chem.* **2008**, *73*, 5048. (f) Fleischhauer, J.; Zahn, S.; Beckert, R.; Grummt, U.-W.; Brickner, E.; Görls, H. *Chem.—Eur. J.* **2012**, *18*, 4549.
(5) Koutentis, P. A.; Re, D. L. *Synthesis* **2010**, *2010*, 2075.
(6) Potts, K. T.; Roy, S. K.; Jones, D. P. *J. Org. Chem.* **1967**, *32*, 2245.
(7) Rotas, G.; Kimbaris, A.; Varvounis, G. *Tetrahedron* **2004**, *60*, 10825.
(8) Berezin, A. A.; Zissimou, G.; Constantinides, C. P.; Beldjoudi, Y.; Rawson, J. M.; Koutentis, P. A. *J. Org. Chem.* **2014**, *79*, 314.
(9) Ioannou, T. A.; Koutentis, P. A.; Krassos, H.; Loizou, G.; Re, D. L. *Org. Biomol. Chem.* **2012**, *10*, 1339.
(10) (a) Haas, Y.; Zilberg, S. *J. Am. Chem. Soc.* **2004**, *126*, 8991.
(11) Schleyer, P. v. R.; Manoharan, M.; Wang, Z.-X.; Kiran, B.; Jiao, H.; Puchta, R.; van Eikema Hommes, N. J. R. *Org. Lett.* **2001**, *3*, 2465.
(12) (a) Constantinides, C. P.; Koutentis, P. A.; Schatz, J. *J. Am. Chem. Soc.* **2004**, *126*, 16232. (b) Constantinides, C. P.; Ioannou, T. A.; Koutentis, P. A. *Polyhedron* **2013**, *64*, 172. (c) Strassner, T.; Weitz, A.; Rose, J.; Wudl, F.; Houk, K. N. *Chem. Phys. Lett.* **2000**, *321*, 459. (d) Braunstein, P.; Siri, O.; Taquet, J.-p.; Rohmer, M.-M.; Bénard, M.; Welter, R. *J. Am. Chem. Soc.* **2003**, *125*, 12246.
(13) Smith, M. B.; Michl, J. *Chem. Rev.* **2010**, *110*, 6891.

DOI: 10.1021/acs.orglett.5b01923
Org. Lett. 2015, 17, 4026−4029